RRKM study and DFT assessment for gas-phase fragmentation of formamide-M^{2+} (M=Ca, Sr)

Ana Martín-Sómer[1], Marie-Pierre Gaigeot[2], Manuel Yáñez[1*] and Riccardo Spezia[2*]

Contribution from [1]Departamento de Química, Facultad de Ciencias, Módulo 13. Universidad Autónoma de Madrid. Cantoblanco, 28049-Madrid. Spain, and [2]Laboratoire Analyse et Modélisation pour la Biologie et l'Environnement (LAMBE), UMR-CNRS 8587, Université d'Evry val d'Essonne, Blvd. F. Mitterrand, Bat. Maupertuis, F-91025 Evry, France.

Supporting Information
(20 pages)
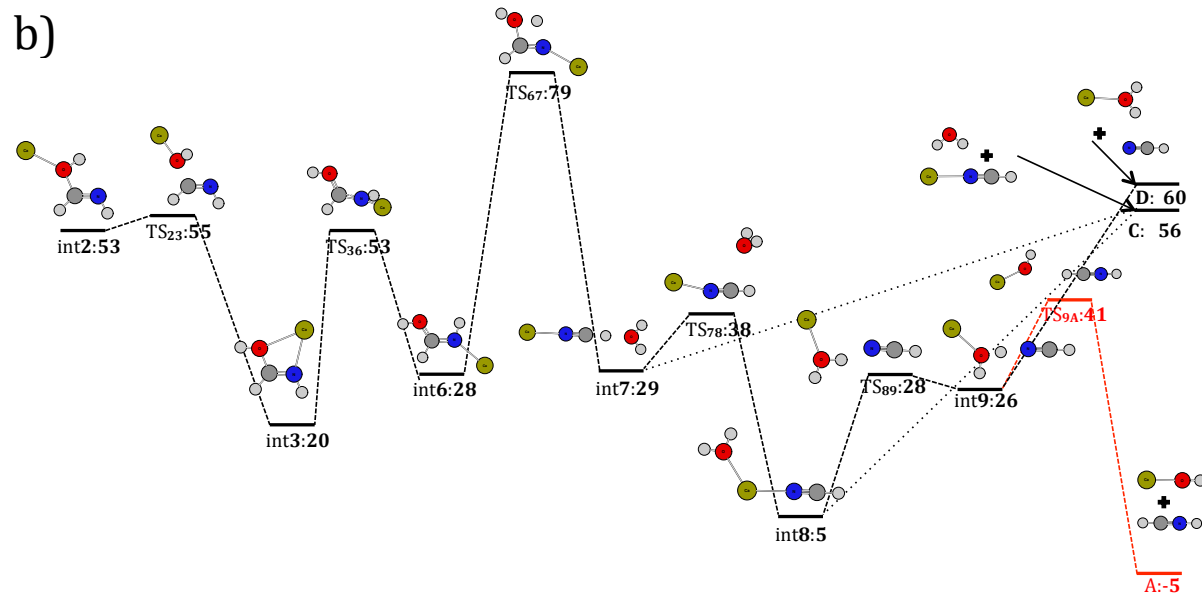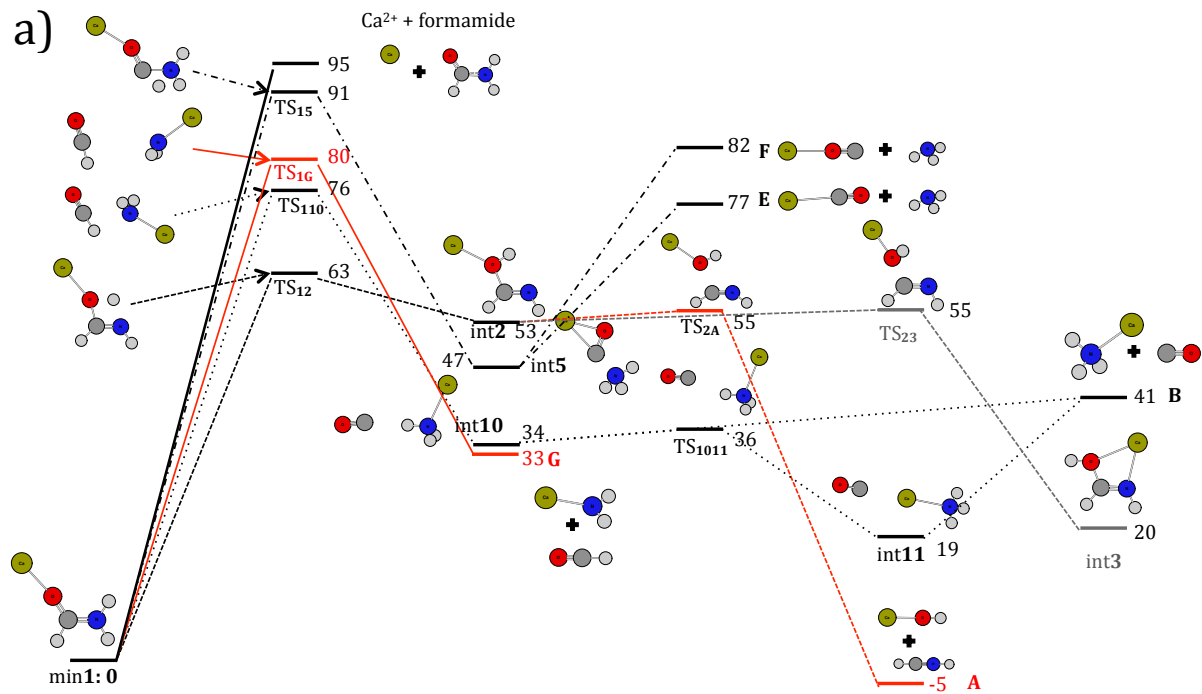
Figure S.1. Energy profile of the different reaction mechanisms with origin in **a)** the global minimum **1** and **b)** the local minimum int**2** for formamide-Ca^{2+}system. All values in kcal/mol.
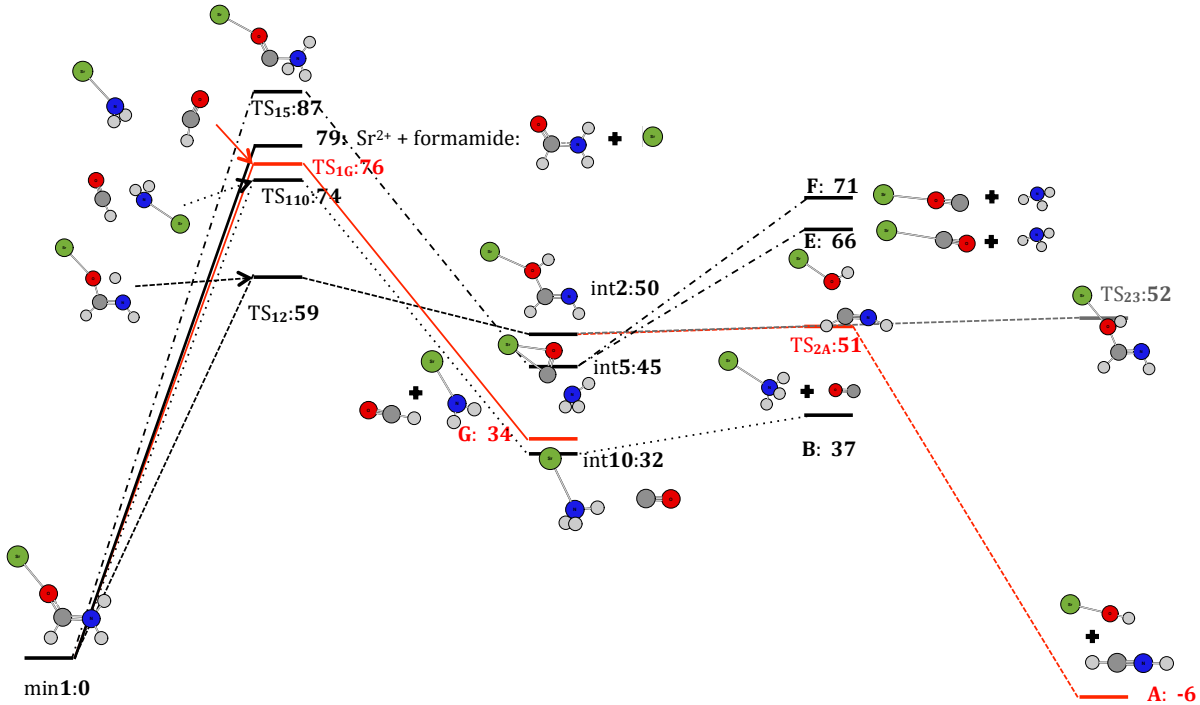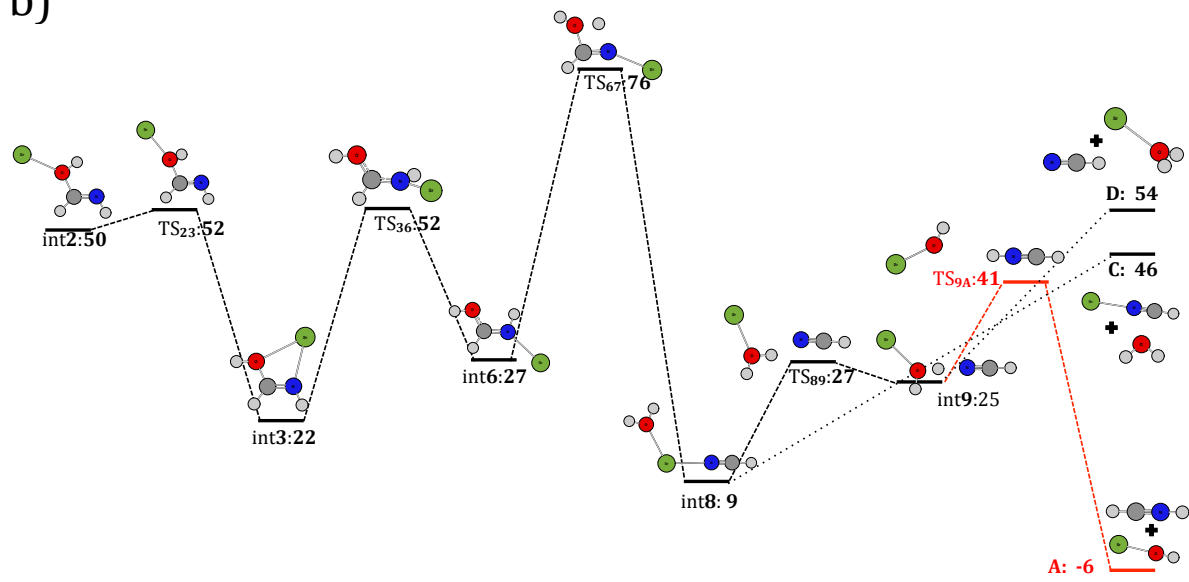
Figure S.2: Energy profile of the different reaction mechanisms with origin in **a)** the global minimum **1** and **b)** the local minimum int**2** for formamide-Sr^{2+} system. All values in kcal/mol.

Rotational constant **A**:

Structure	B3LYP/6-31G(d)	G96LYP/6-31G(d)	MP2/6-31G(d)	BLYP/6-31G(d)
Formamide	-0.9	-2.4	-1.9	-2.8
A_CaOH$^+$	0.0	0.0	0.0	0.0
A_HCNH$^+$	0.0	0.0	0.0	0.0
B_CaNH$_3^{2+}$	-0.2	-1.4	0.1	-1.8
B_CO	0.0	0.0	0.0	0.0
C_CaHCN^{2+}	0.0	0.0	0.0	0.0
C_H$_2$O	-3.4	-6.7	-2.7	-7.6
D_CaH$_2$O^{2+}	-0.1	-1.4	-0.1	-1.7
D_HCN	0.0	0.0	0.0	0.0
E_CaCO^{2+}	0.0	0.0	0.0	0.0
E_NH$_3$	-1.9	-4.0	-1.0	-4.4
F_CaOC^{2+}	0.0	0.0	0.0	0.0
F_NH$_3$	-1.9	-4.0	-1.0	-4.4
G_CaNH$_2^+$	-6.3	-13.6	-0.1	-16.3
G_OCH$^+$	0.0	0.0	0.0	0.0
int_10	1.3	2.8	-2.7	1.5
int_11	0.0	-1.3	0.2	-1.9
int_1	0.4	0.1	2.2	0.1
int_2	-0.5	-2.7	-0.2	-3.1
int_3	-1.3	-2.6	-1.7	-3.0
int_5	-0.3	-4.7	-3.6	-4.9
int_6	-0.6	-2.9	-1.5	-3.4
int_7	-14.0	-31.5	0.7	-33.2
int_8	2683.2	2673.1	2689.3	2642.1
int_9	-15.0	-10.6	-26.4	-11.8
TS_10_11	0.0	-2.7	6.1	-1.1
TS_1_10	-2.7	-9.6	-0.6	-9.5
TS_1_1	-1.6	-3.5	-2.3	-4.0
TS_1_2	0.0	-1.1	-1.6	-1.2
TS_1_5	1.8	-0.8	0.4	-1.3
TS_1_G	3.4	-5.0	29.4	-3.1
TS_2_3	-8.9	-13.7	-11.0	-14.4
TS_2_A	1.4	-0.8	1.4	-1.0
TS_3_6	-8.8	-11.6	-9.0	-12.4
TS_6_7	0.0	-2.7	-0.5	-2.0
TS_7_8	-3.1	-5.7	1.9	0.1
TS_8_9	4.5	-2.4	10.8	0.7
TS_9_A	18.5	33.7	21.7	67.0

Table S.1-a : Relative errors (%) in C rotational constant. M=Ca.

Rotational constant **B**:

Structure	B3LYP/6-31G(d)	G96LYP/6-31G(d)	MP2/6-31G(d)	BLYP/6-31G(d)
Formamide	-0.9	-2.7	-1.2	-2.8
A_CaOH$^+$	-9.0	-9.7	-9.9	-10.1
A_HCNH$^+$	-1.5	-3.0	-3.3	-3.1
B_CaNH$_3^{2+}$	-6.2	-7.5	-7.3	-7.6
B_CO	-2.2	-4.2	-4.5	-4.3
C_CaHCN^{2+}	-5.3	-6.6	-7.6	-6.4
C_H$_2$O	-0.3	-1.2	-0.7	-1.2
D_CaH$_2$O^{2+}	-5.2	-6.5	-6.7	-6.3
D_HCN	-1.8	-3.6	-4.6	-3.7
E_CaCO^{2+}	-4.4	-5.8	-5.7	-5.2
E_NH$_3$	-1.8	-3.9	-0.9	-4.3
F_CaOC^{2+}	-3.3	-5.6	-6.0	-5.0
F_NH$_3$	-1.8	-3.9	-0.9	-4.3
G_CaNH$_2^+$	-11.4	-14.1	-11.0	-15.2
G_OCH$^+$	-2.0	-3.8	-4.5	-4.0
int_10	-4.2	-6.3	-6.4	-4.7
int_11	0.0	-1.4	-0.9	-1.2
int_1	-4.6	-6.0	-5.7	-6.0
int_2	-3.1	-4.7	-4.1	-4.9
int_3	-4.5	-6.6	-5.3	-6.1
int_5	-6.3	-9.7	-6.1	-9.6
int_6	-4.9	-6.1	-6.1	-6.1
int_7	-4.2	-4.5	-7.9	-4.4
int_8	-24.3	-25.3	-25.7	-25.1
int_9	-3.8	-5.5	-4.4	-5.1
TS_10_11	0.0	-0.9	-7.2	0.0
TS_1_10	1.2	0.6	-1.0	0.0
TS_1_1	-5.4	-6.7	-6.7	-6.7
TS_1_2	-4.0	-5.6	-4.9	-5.6
TS_1_5	-4.3	-5.8	-5.0	-5.6
TS_1_G	-13.0	-9.2	27.3	-11.9
TS_2_3	-0.6	-1.1	-0.9	-1.1
TS_2_A	-1.3	-5.1	-4.9	-5.7
TS_3_6	-3.0	-3.8	-3.8	-3.7
TS_6_7	-5.5	-6.9	-7.1	-7.1
TS_7_8	-2.0	-1.6	-11.7	-3.3
TS_8_9	-9.9	-7.3	-16.5	-8.8
TS_9_A	-22.1	-21.1	-21.7	-24.2

Table S.1-b : Relative errors (%) in B rotational constant. M=Ca.

Rotational constant C:

Structure	B3LYP/6-31G(d)	G96LYP/6-31G(d)	MP2/6-31G(d)	BLYP/6-31G(d)
Formamide	-0.9	-2.7	-1.2	-2.8
A_CaOH$^+$	-9.0	-9.7	-9.9	-10.1
A_HCNH$^+$	-1.5	-3.0	-3.3	-3.1
B_CaNH$_3^{2+}$	-6.2	-7.5	-7.3	-7.6
B_CO	-2.2	-4.2	-4.5	-4.3
C_CaHCN^{2+}	-5.3	-6.6	-7.6	-6.4
C_H$_2$O	-1.4	-3.2	-1.4	-3.5
D_CaH$_2$O^{2+}	-5.1	-6.4	-6.6	-6.2
D_HCN	-1.8	-3.6	-4.6	-3.7
E_CaCO^{2+}	-4.4	-5.8	-5.7	-5.2
E_NH$_3$	0.0	-0.8	-0.3	-0.7
F_CaOC^{2+}	-3.3	-5.6	-6.0	-5.0
F_NH$_3$	0.0	-0.8	-0.3	-0.7
G_CaNH$_2^+$	-11.0	-13.6	-10.8	-14.6
G_OCH$^+$	-2.0	-3.8	-4.5	-4.0
int_10	-3.9	-5.7	-6.1	-4.3
int_11	0.0	-1.4	-0.9	-1.2
int_1	-4.4	-5.8	-5.4	-5.8
int_2	-3.1	-4.7	-4.0	-4.8
int_3	-3.7	-5.6	-4.4	-5.3
int_5	-5.8	-9.3	-5.9	-9.3
int_6	-4.8	-6.0	-6.0	-6.1
int_7	-4.2	-4.4	-7.9	-4.3
int_8	-14.8	-16.0	-16.4	-15.8
int_9	-4.3	-5.7	-5.6	-5.4
TS_10_11	0.0	-1.1	-5.7	-0.1
TS_1_10	1.2	0.7	-1.0	0.0
TS_1_1	-4.5	-6.0	-5.7	-6.0
TS_1_2	-3.9	-5.4	-4.7	-5.5
TS_1_5	-4.2	-5.6	-4.9	-5.5
TS_1_G	-12.1	-8.6	27.6	-11.0
TS_2_3	-1.3	-2.3	-1.9	-2.4
TS_2_A	-1.3	-5.1	-4.8	-5.6
TS_3_6	-3.5	-4.4	-4.2	-4.3
TS_6_7	-5.2	-6.6	-6.8	-6.8
TS_7_8	-2.2	-2.3	-9.7	-2.7
TS_8_9	-8.3	-6.8	-13.9	-7.7
TS_9_A	-21.8	-20.7	-21.3	-23.6

Table S.1-c : Relative errors (%) in C rotational constant. M=Ca.

Rotational constant **A**:

Structure	B3LYP/6-31G(d)	G96LYP/6-31G(d)	MP2/6-31G(d)
Formamide	2.1	0.6	1.0
A_HCNH$^+$	0.0	0.0	0.0
A_SrOH$^+$	0.0	0.0	0.0
B_CO	0.0	0.0	0.0
B_SrNH$_3$$^{2+}$	2.2	1.0	2.3
C_H$_2$O	-2.1	-5.2	-1.4
C_HCNSr^{2+}	-3.2	-7.9	-10.1
D_HCN	0.0	0.0	0.0
D_Sr-H$_2$O^{2+}	2.8	1.7	2.7
E_NH$_3$	-0.3	-2.3	0.6
E_OC-Sr^{2+}	0.0	0.0	0.0
F_CO-Sr^{2+}	0.0	0.0	0.0
F_NH$_3$	-0.3	-2.3	0.6
G_SrNH$_2$$^+$	-6.1	-11.2	2.4
G_OCH$^+$	0.0	0.0	0.0
min1	6.2	5.9	9.4
int2	2.8	0.5	3.8
int3	0.9	0.0	0.1
int6	2.9	1.0	2.8
int8	159.2	1184.1	4998.3
int9	-13.8	-12.0	-29.3
int10	20.4	17.6	14.1
int5	4.7	-4.4	2.6
TS_1_1	0.7	-1.4	0.0
TS_1_2	2.5	1.6	0.7
TS_1_10	14.6	2.7	20.3
TS_1_5	3.1	-0.6	1.7
TS_2_3	-5.3	-11.6	-6.4
TS_2_A	19.3	18.0	20.9
TS_3_6	-4.5	-7.3	-6.3
TS_6_8	3.9	0.1	3.4
TS_8_9	27.0	15.3	28.7
TS_9_A	169.4	179.0	96.7
TS_1_G	13.2	2.7	268.4

Table S.2-a: Relative errors (%) in A rotational constant. M=Sr.

Rotational constant **B**:

Structure	B3LYP/6-31G(d)	G96LYP/6-31G(d)	MP2/6-31G(d)
Formamide	1.7	-0.1	1.4
A_HCNH$^+$	1.6	0.0	-0.3
A_SrOH$^+$	-6.9	-8.2	-7.6
B_CO	1.9	-0.1	-0.4
B_SrNH$_3$$^{2+}$	-3.5	-4.8	-5.3
C_H$_2$O	3.0	2.0	2.6
C_HCNSr^{2+}	-3.6	-5.0	-6.4
D_HCN	1.9	0.0	-1.1
D_Sr-H$_2$O^{2+}	-3.4	-4.9	-5.1
E_NH$_3$	-0.3	-2.3	0.6
E_OC-Sr^{2+}	-3.0	-4.6	-5.0
F_CO-Sr^{2+}	-2.9	-6.2	-6.1
F_NH$_3$	-0.3	-2.3	0.6
G_SrNH$_2$$^+$	-10.1	-12.7	-10.8
G_OCH$^+$	1.9	0.0	-0.8
min1	-3.6	-5.1	-5.1
int2	-1.6	-3.4	-3.2
int3	-3.1	-6.9	-3.7
int6	-2.5	-3.8	-4.6
int8	-19.0	-26.1	-27.7
int9	-3.0	-4.7	-2.4
int10	-7.1	-8.2	-9.4
int5	-5.7	-11.2	-5.9
TS_1_1	-3.7	-5.4	-5.7
TS_1_2	-2.3	-4.1	-3.5
TS_1_10	1.9	1.4	-0.3
TS_1_5	-1.1	-2.9	-2.7
TS_2_3	0.7	0.6	-0.8
TS_2_A	6.9	4.1	4.7
TS_3_6	-1.8	-2.7	-2.7
TS_6_8	-3.6	-4.9	-5.8
TS_8_9	-18.5	-16.0	-22.4
TS_9_A	-24.0	-23.4	-23.5
TS_1_G	-14.6	-10.5	-5.5

Table S.2-b: Relative errors (%) in A rotational constant. M=Sr.

Rotational constant **C**:

Structure	B3LYP/6-31G(d)	G96LYP/6-31G(d)	MP2/6-31G(d)
Formamide	1.8	0.0	1.5
A_HCNH$^+$	1.6	0.0	-0.3
A_SrOH$^+$	-6.9	-8.2	-7.6
B_CO	1.9	-0.1	-0.4
B_SrNH$_3$$^{2+}$	-3.5	-4.8	-5.3
C_H$_2$O	1.2	-0.6	1.2
C_HCNSr^{2+}	-3.6	-5.0	-6.4
D_HCN	1.9	0.0	-1.1
D_Sr-H$_2$O^{2+}	-3.3	-4.9	-5.0
E_NH$_3$	3.2	2.4	2.8
E_OC-Sr^{2+}	-3.0	-4.6	-5.0
F_CO-Sr^{2+}	-2.9	-6.2	-6.1
F_NH$_3$	3.2	2.4	2.8
G_SrNH$_2$$^+$	-9.7	-12.3	-10.6
G_OCH$^+$	1.9	0.0	-0.8
min1	-3.3	-4.9	-4.7
int2	-1.5	-3.3	-3.1
int3	-2.4	-5.8	-3.1
int6	-2.4	-3.7	-4.4
int8	-7.8	-11.5	-13.2
int9	-3.5	-5.0	-3.7
int10	-5.5	-6.7	-8.0
int5	-5.2	-10.9	-5.5
TS_1_1	-3.0	-4.8	-4.8
TS_1_2	-2.2	-3.9	-3.4
TS_1_10	1.8	1.4	-0.4
TS_1_5	-1.1	-2.8	-2.7
TS_2_3	0.3	-0.3	-1.3
TS_2_A	6.4	3.7	4.4
TS_3_6	-2.0	-3.0	-3.0
TS_6_8	-3.3	-4.7	-5.5
TS_8_9	-15.0	-13.3	-18.6
TS_9_A	-23.3	-22.6	-22.8
TS_1_G	-13.8	-10.0	-2.5

Table S.2-c: Relative errors (%) in C rotational constant. M=Sr.

	Absolute error (kcal/mol)				Relative error(%)			
Structure	B3LYP[a]	G96LYP [a]	MP2 [a]	BLYP [a]	B3LYP [a]	G96LYP [a]	MP2 [a]	BLYP [a]
Form/Ca^{2+}	6.59	11.15	9.23	7.22	-6.9	-11.7	-9.7	-7.6
A	25.29	21.07	17.28	20.89	-528.6	-440.5	-361.2	-436.6
B	1.28	4.97	10.51	2.64	-3.1	-12.1	-25.5	-6.4
C	2.35	1.54	9.93	0.73	4.2	-2.7	-17.6	1.3
D	1.64	2.71	12.32	0.38	2.7	-4.5	-20.4	-0.6
E	1.16	6.22	11.60	3.91	-1.5	-8.0	-15.0	-5.0
F	2.51	5.65	9.43	3.22	-3.1	-6.9	-11.5	-3.9
G	19.41	12.64	13.67	11.43	58.4	38.0	41.1	34.4
int10	2.51	4.97	11.50	4.93	-7.3	-14.5	-33.6	-14.4
int11	4.03	6.15	13.79	6.67	-21.1	-32.2	-72.1	-34.8
min1	0.00	0.00	0.00	0.00	0.0	0.0	0.0	0.0
int2	2.00	3.75	4.72	4.50	-3.8	-7.1	-8.9	-8.5
int3	2.49	2.06	5.05	2.75	-12.1	-10.0	-24.6	-13.3
int4	0.72	2.53	2.41	3.33	-1.3	-4.5	4.3	-6.0
int5	0.94	3.04	2.59	3.99	-2.0	-6.5	-5.5	-8.5
int6	0.45	1.59	0.16	1.63	-1.6	-5.6	-0.6	-5.8
int7	4.33	1.93	5.30	2.25	14.7	6.5	-18.0	7.6
int8	1.65	0.81	10.63	0.36	31.3	15.3	-201.9	6.9
int9	4.41	2.02	7.20	1.84	16.6	7.6	-27.1	6.9
TS_10_11	4.20	6.56	13.48	6.58	-11.6	-18.2	-37.3	-18.2
TS_1_10	4.95	1.23	2.28	2.90	6.5	-1.6	3.0	-3.8
TS_1_1	4.85	4.55	7.04	5.51	-16.7	-15.7	-24.3	-19.0
TS_1_2	0.86	4.72	3.61	4.93	-1.4	-7.5	-5.7	-7.8
TS_1_5	1.10	3.72	3.08	4.23	1.2	-4.1	3.4	-4.6
TS_1_G	12.67	2.31	7.72	1.61	15.9	2.9	9.7	2.0
TS_2_3	1.71	3.22	4.33	3.86	-3.1	-5.9	-7.9	-7.0
TS_2_A	5.06	0.89	1.56	0.34	9.2	1.6	2.8	-0.6
TS_3_6	2.41	1.06	5.02	0.76	4.5	2.0	9.5	1.4
TS_6_7	2.14	2.59	0.40	2.97	2.7	-3.3	0.5	-3.8
TS_7_8	4.00	2.23	7.61	1.99	10.4	5.8	-19.8	5.2
TS_8_9	3.34	1.45	8.66	1.13	11.8	5.1	-30.7	4.0
TS_9_A	19.23	15.20	11.01	14.65	47.0	37.2	26.9	35.8

a) 6-31G(d) basis set

Table S.3: Absolute and relative errors (%) for relative energies computed with the four trial methods. M=Ca.

| Structure	Absolute error (kcal/mol)				Relative error(%)			
	B3LYP [a)]	G96LYP [a)]	MP2 [a)]	G96LYP [b)]	B3LYP [a)]	G96LYP [a)]	MP2 [a)]	G96LYP [b)]
Form/Sr^{2+}	13.25	18.74	16.41	6.14	-16.7	-23.6	-20.7	-7.7
A	45.16	40.10	37.33	7.14	-755.1	-670.4	-624.2	-119.4
B	4.80	9.05	14.61	2.29	-12.9	-24.4	-39.4	-6.2
C	4.93	0.76	8.09	0.78	10.8	1.7	-17.7	1.7
D	0.33	5.21	15.29	2.74	-0.6	-9.6	-28.3	-5.1
E	2.23	7.67	12.44	0.02	-3.4	-11.6	-18.8	0.0
F	4.32	8.00	11.97	1.44	-6.1	-11.2	-16.8	-2.0
G	33.58	25.21	31.59	9.29	99.9	75.0	94.0	27.6
min1	0.00	0.00	0.00	0.00	0.0	0.0	0.0	0.0
int2	3.96	5.50	6.26	1.03	-8.0	-11.1	-12.6	-2.1
int3	5.45	5.20	6.66	1.07	-24.5	-23.4	-29.9	-4.8
int6	2.97	4.25	2.11	0.01	-10.8	-15.4	-7.7	0.0
int8	1.23	0.18	11.04	0.81	13.2	1.9	-118.3	8.7
int9	3.58	1.42	8.27	0.33	14.4	5.7	-33.2	1.3
int10	5.11	7.74	13.22	0.00	-16.0	-24.3	-41.5	0.0
int5	0.56	2.57	0.09	1.16	1.2	-5.7	0.2	2.6
TS_1_1	6.23	5.86	7.45	0.03	-21.0	-19.8	-25.1	-0.1
TS_1_2	0.32	4.23	2.46	1.74	-0.5	-7.2	-4.2	-2.9
TS_1_10	9.64	2.83	9.81	3.20	13.0	3.8	13.3	4.3
TS_1_5	4.38	0.81	6.75	0.41	5.0	-0.9	7.8	-0.5
TS_2_3	3.89	5.12	6.06	1.09	-7.5	-9.9	-11.7	-2.1
TS_2_A	6.99	3.97	5.59	2.01	13.6	7.7	10.9	3.9
TS_3_6	2.00	0.37	5.54	0.92	3.8	0.7	10.6	1.8
TS_6_8	3.02	1.94	1.73	0.96	4.0	-2.5	2.3	-1.3
TS_8_9	2.15	0.21	9.95	0.56	8.1	0.8	-37.5	2.1
TS_9_A	35.87	31.39	28.58	5.49	87.7	76.7	69.9	13.4
TS_1_G	25.91	11.99	26.88	5.59	34.1	15.8	35.4	7.3

a) 6-31G(d) basis set
b) 6-31+G(d,p) basis set

Table S.4: Absolute and relative errors (%) for relative energies computed with the four trial methods. M=Sr.
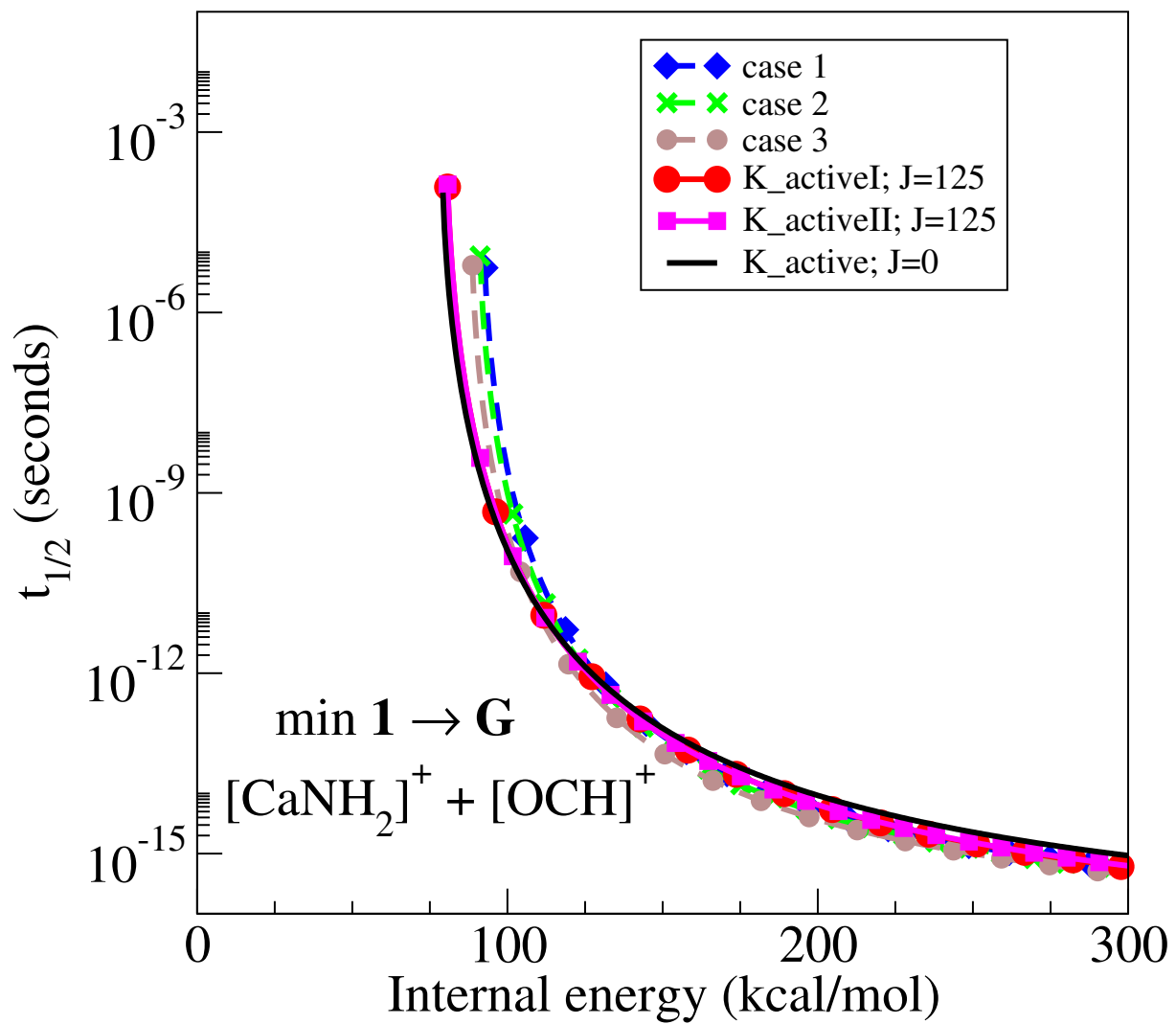
Figure S.3-a: k(E) computed at B3LYP/cc-pWCVTZ for min**1**→ **G** ([CaNH₂]⁺ + [HCO]⁺) reaction (M=Ca), taking into account the rotational energy. The quantum *K* number can be treated as an active rotor (solid lines) with different values for the angular moment J; or as an adiabatic rotor (dashed lines), where all the rotational energy is placed on the *x,y*-axes (blue diamonds, dashed line)(*case1*) ; equally distributed among the three axes (green crosses, dashed line) (*case2*) or in the *z*-axis (brown circles, dashed line) (*case3*).
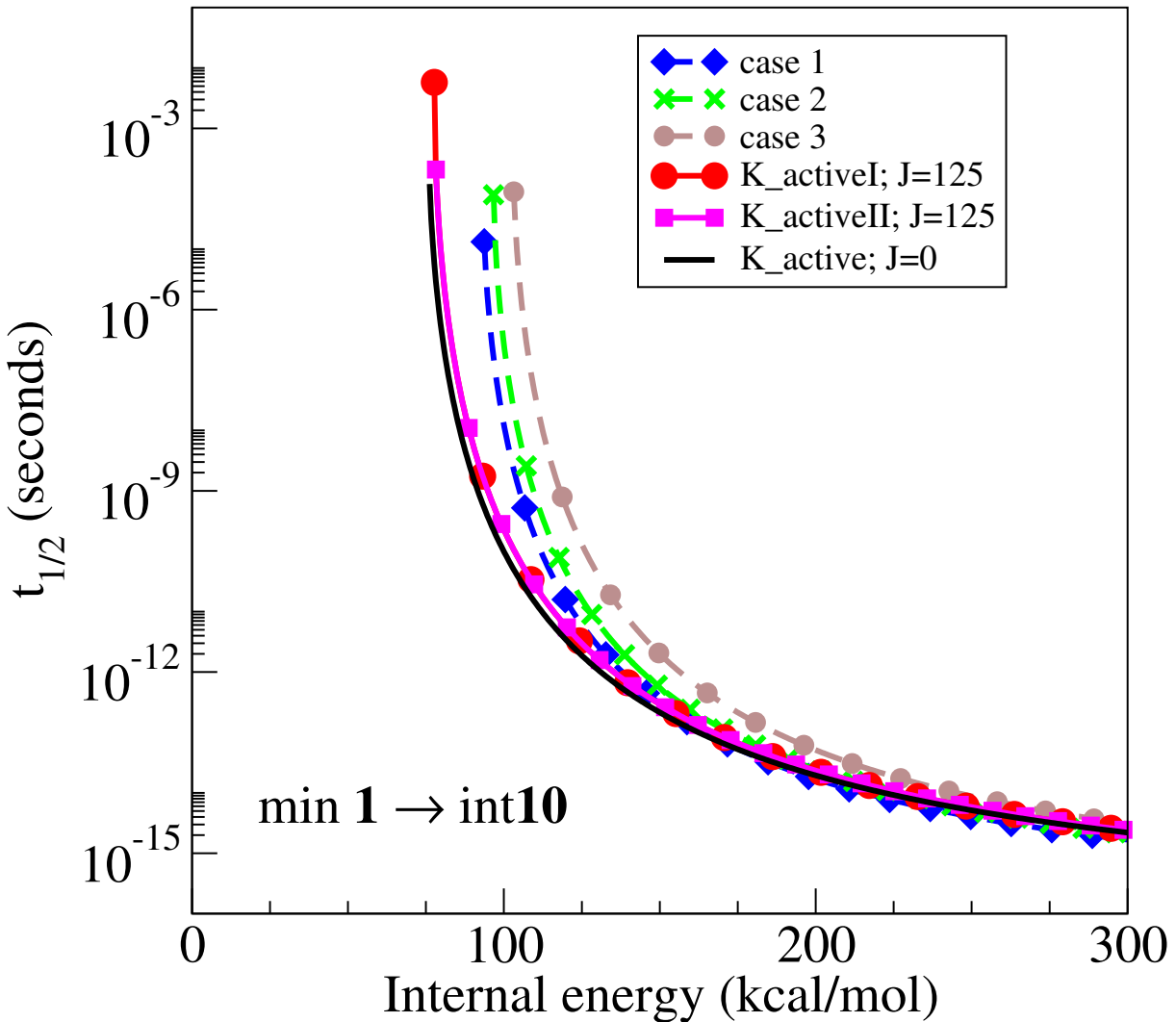
Figure S.3-b: k(E) computed at B3LYP/cc-pWCVTZ for min**1**→ int**10** reaction (M=Ca), taking into account the rotational energy. The quantum *K* number can be treated as an active rotor (solid lines) with different values for the angular moment J; or as an adiabatic rotor (dashed lines), where all the rotational energy is placed on the *x,y*-axes (blue diamonds, dashed line)(*case1*) ; equally distributed among the three axes (green crosses, dashed line) (*case2*) or in the *z*-axis (brown circles, dashed line) (*case3*).
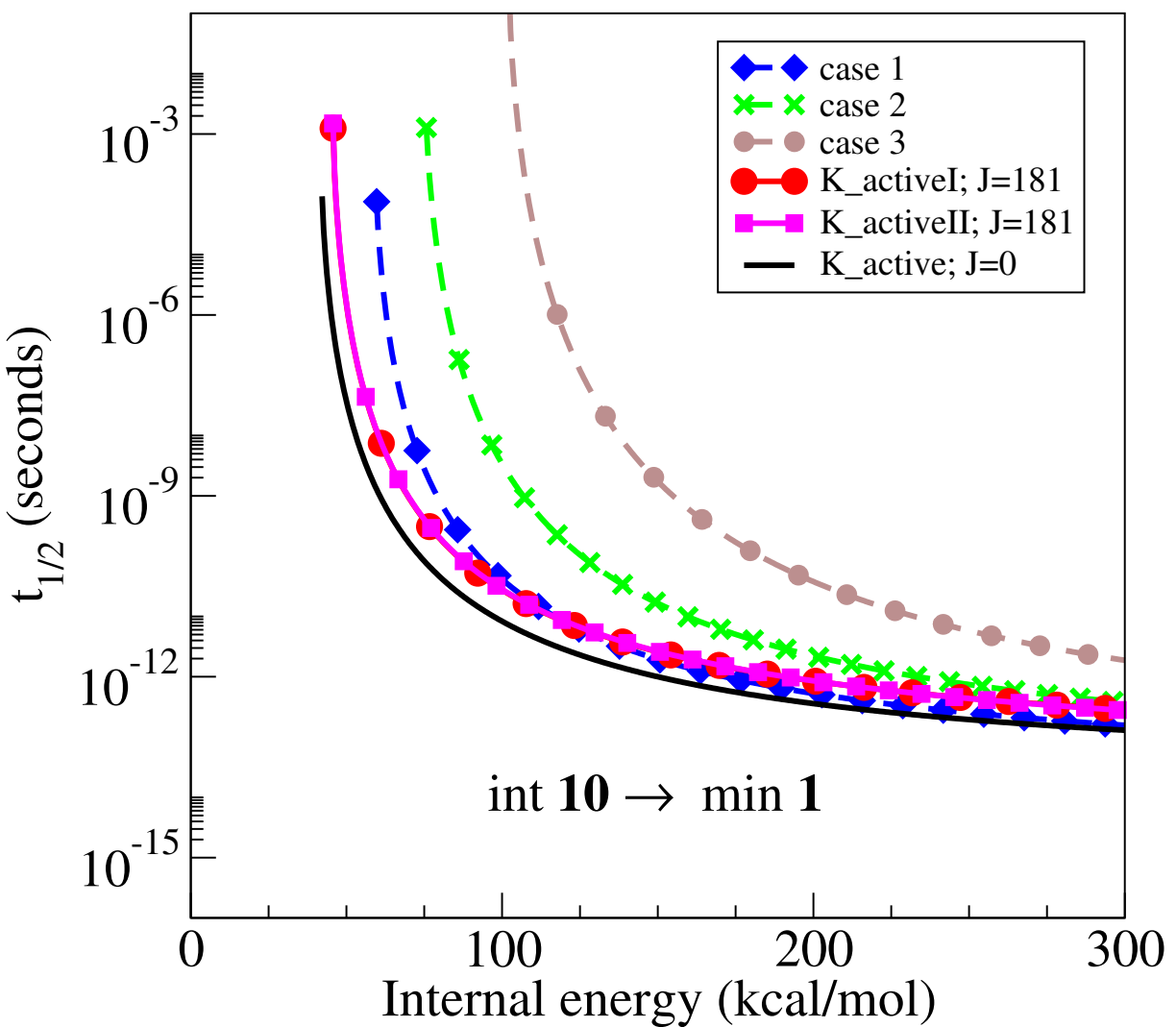
Figure S.3-c: k(E) computed at B3LYP/cc-pWCVTZ for int**10**→ min**1** reaction (M=Ca), taking into account the rotational energy. The quantum K number can be treated as an active rotor (solid lines) with different values for the angular moment J; or as an adiabatic rotor (dashed lines), where all the rotational energy is placed on the *x,y*-axes (blue diamonds, dashed line)(*case1*) ; equally distributed among the three axes (green crosses, dashed line) (*case2*) or in the *z*-axis (brown circles, dashed line) (*case3*).
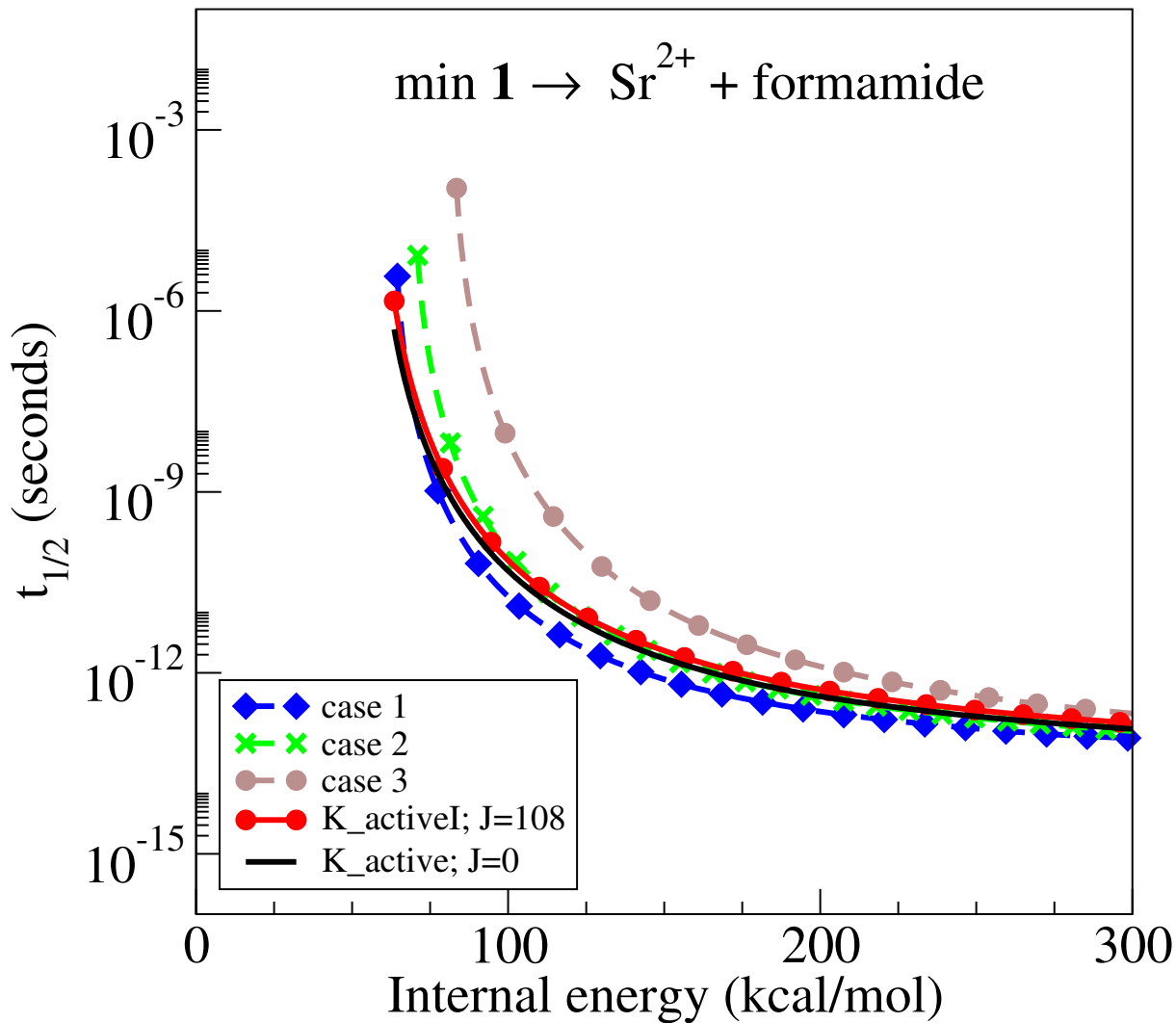
Figure S.3-d: k(E) computed at G96LYP/6-311+G(3df.2p) for min**1** → Sr^{2+} + formamide reaction (M=Sr), taking into account the rotational energy. The quantum K number can be treated as an active rotor (solid lines) with different values for the angular moment J; or as an adiabatic rotor (dashed lines), where all the rotational energy is placed on the *x,y*-axes (blue diamonds, dashed line)(*case1*) ; equally distributed among the three axes (green crosses,dashed line) (*case2*) or in the *z*-axis (brown circles, dashed line) (*case3*).
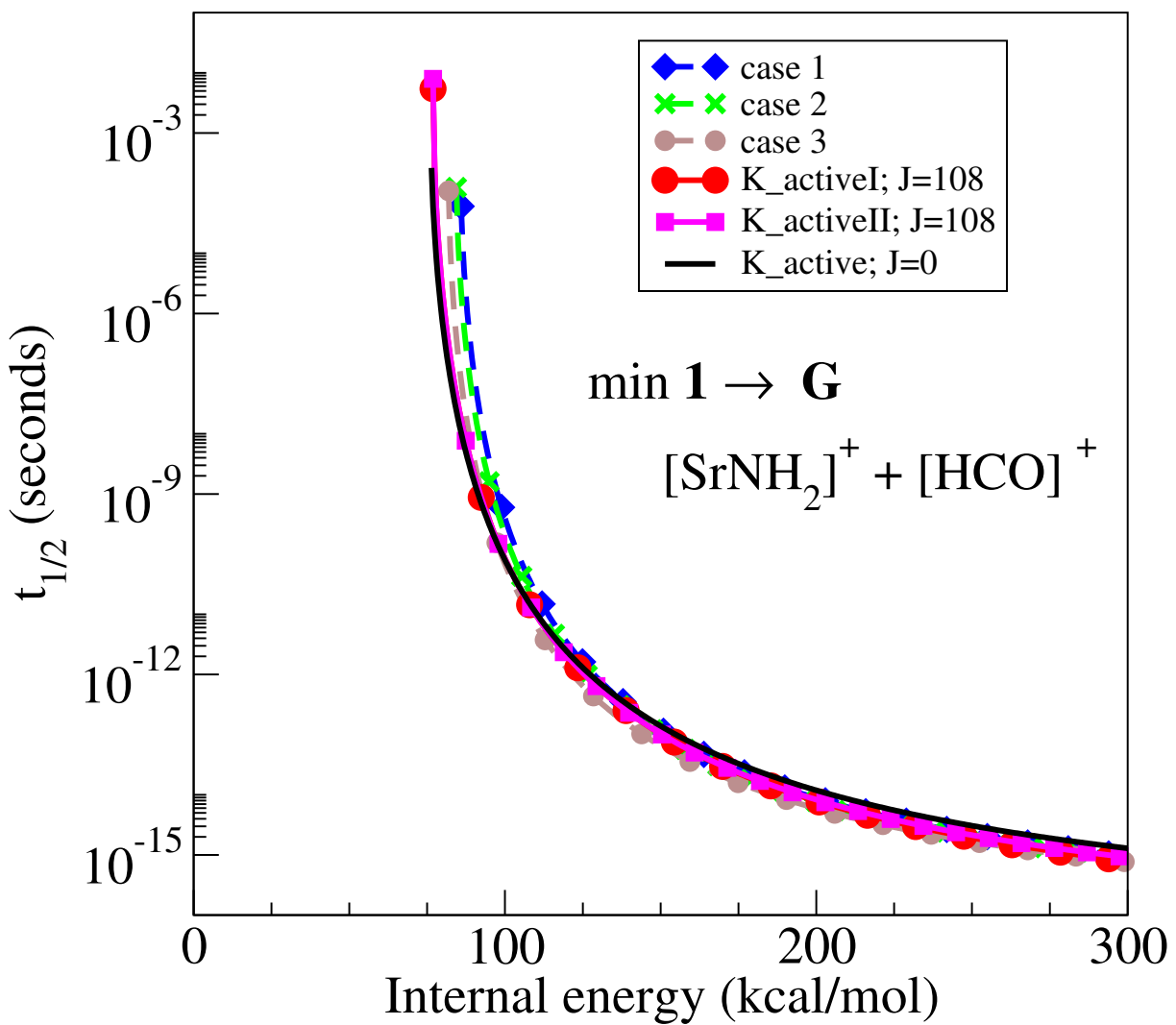
Figure S.3-e: k(E) computed at G96LYP/6-311+G(3df.2p) for min**1** → **G** ([SrNH$_2$]$^+$ + [HCO]$^+$) reaction (M=Sr), taking into account the rotational energy. The quantum *K* number can be treated as an active rotor (solid lines) with different values for the angular moment J; or as an adiabatic rotor (dashed lines), where all the rotational energy is placed on the *x,y*-axes (blue diamonds, dashed line)(*case1*) ; equally distributed among the three axes (green crosses, dashed line) (*case2*) or in the *z*-axis (brown circles, dashed line) (*case3*).
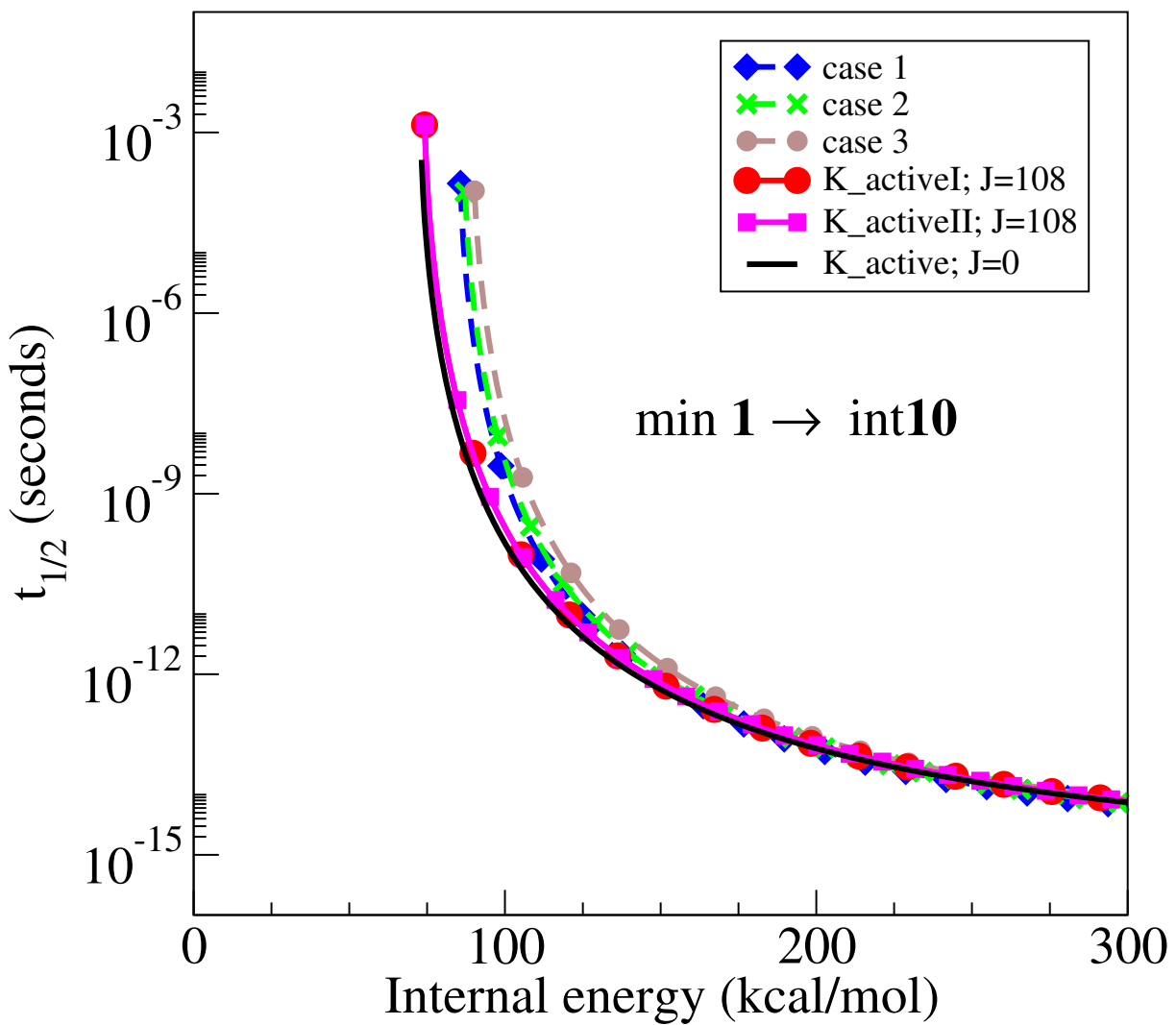
Figure S.3-f: k(E) computed at G96LYP/6-311+G(3df.2p) for min**1** → int**10** reaction (M=Sr), taking into account the rotational energy. The quantum *K* number can be treated as an active rotor (solid lines) with different values for the angular moment J; or as an adiabatic rotor (dashed lines), where all the rotational energy is placed on the *x,y*-axes (blue diamonds, dashed line)(*case1*) ; equally distributed among the three axes (green crosses, dashed line) (*case2*) or in the *z*-axis (brown circles, dashed line) (*case3*).
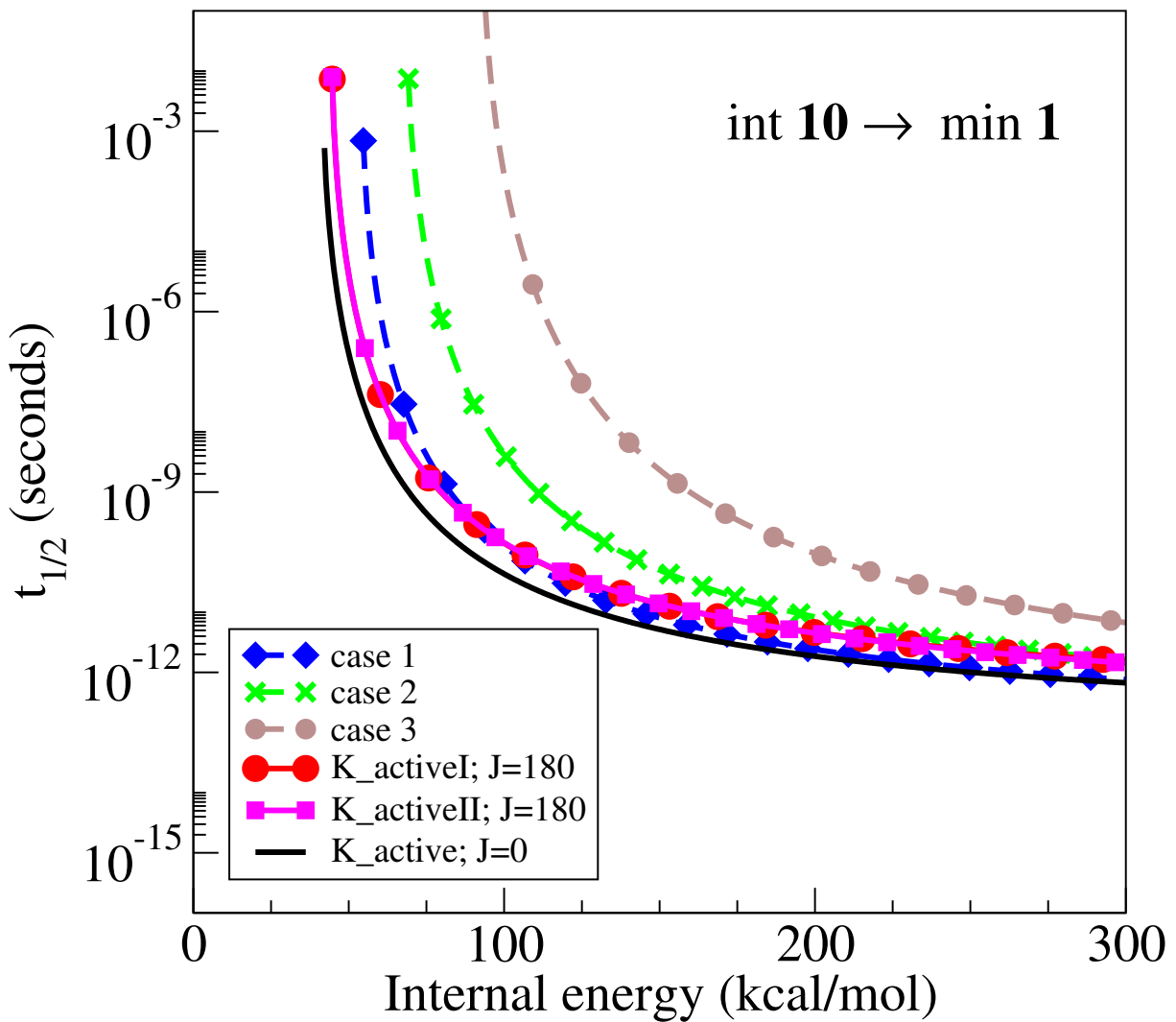
Figure S.3-g: k(E) computed at G96LYP/6-311+G(3df.2p) for int**10** → min**1** reaction (M=Sr), taking into account the rotational energy. The quantum *K* number can be treated as an active rotor (solid lines) with different values for the angular moment J; or as an adiabatic rotor (dashed lines), where all the rotational energy is placed on the *x,y*-axes (blue diamonds, dashed line)(*case1*) ; equally distributed among the three axes (green crosses, dashed line) (*case2*) or in the *z*-axis (brown circles, dashed line) (*case3*).
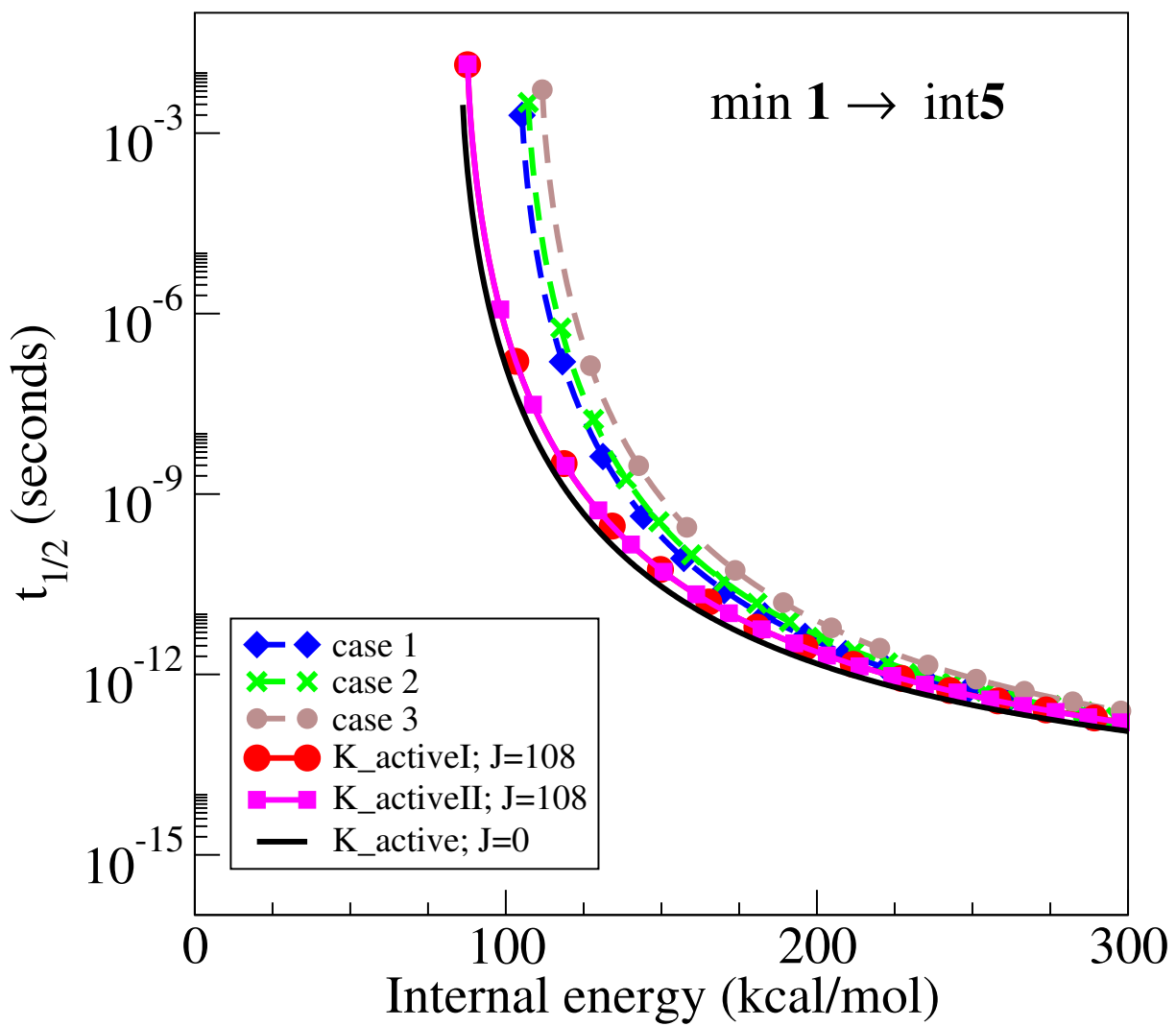
Figure S.3-h: k(E) computed at G96LYP/6-311+G(3df.2p) for min**1** → int**5** reaction (M=Sr), taking into account the rotational energy. The quantum *K* number can be treated as an active rotor (solid lines) with different values for the angular moment J; or as an adiabatic rotor (dashed lines), where all the rotational energy is placed on the *x,y*-axes (blue diamonds, dashed line)(*case1*) ; equally distributed among the three axes (green crosses, dashed line) (*case2*) or in the *z*-axis (brown circles, dashed line) (*case3*).
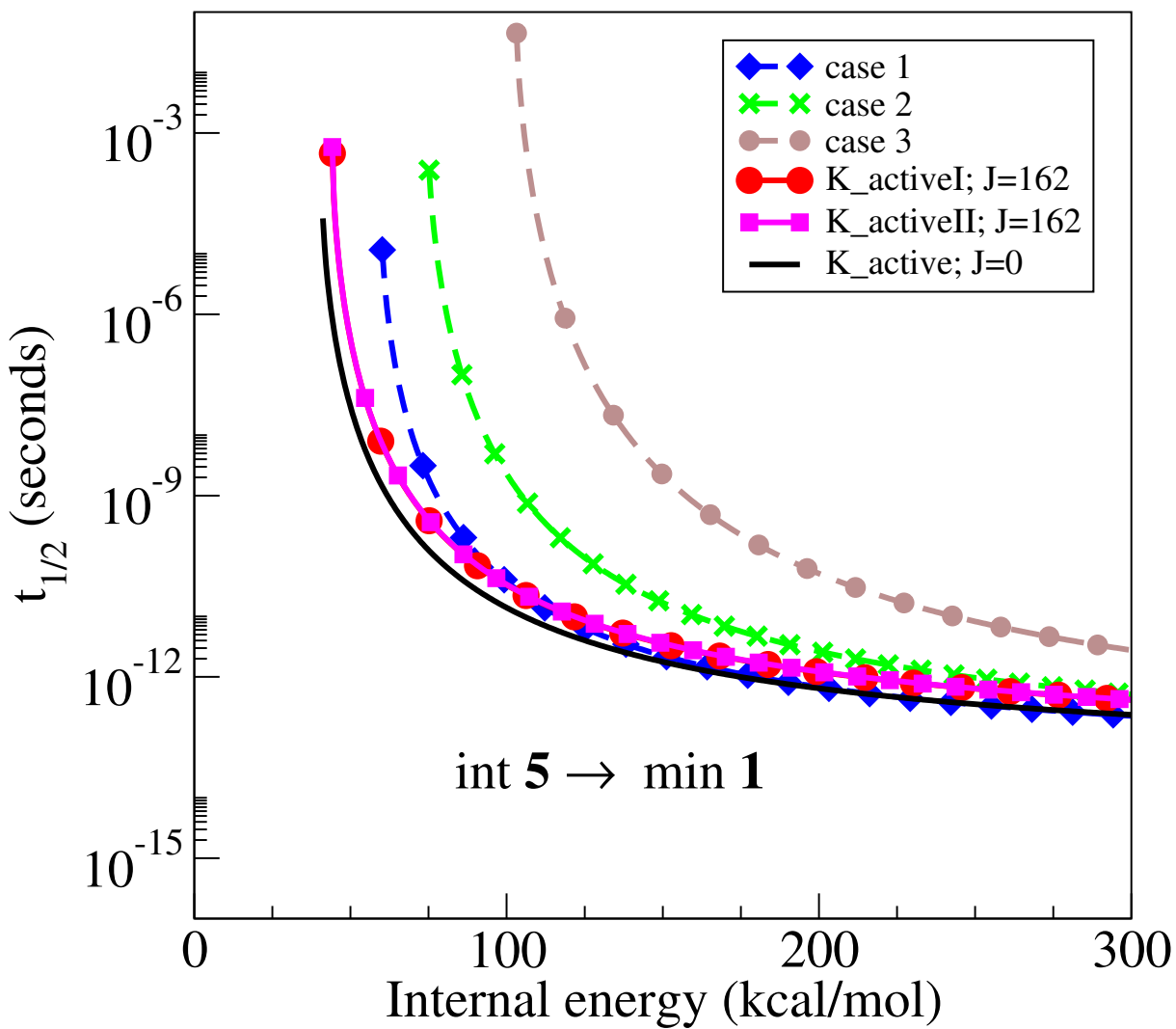
Figure S.3-i: k(E) computed at G96LYP/6-311+G(3df.2p) for int**5** → min**1** reaction (M=Sr), taking into account the rotational energy. The quantum *K* number can be treated as an active rotor (solid lines) with different values for the angular moment J; or as an adiabatic rotor (dashed lines), where all the rotational energy is placed on the *x,y*-axes (blue diamonds, dashed line)(*case1*) ; equally distributed among the three axes (green crosses, dashed line) (*case2*) or in the *z*-axis (brown circles, dashed line) (*case3*).